ELSEVIER

International Journal of Heat and Fluid Flow 21 (2000) 717–726

International Journal of
HEAT AND
FLUID FLOW

www.elsevier.com/locate/ijhff

Warm up of an automotive catalyst substrate by pulsating flow: a single channel modelling approach

S.F. Benjamin, C.A. Roberts *

School of Engineering, Coventry University, Priory Street, Coventry CV1 5FB, UK

Received 26 February 1999; accepted 29 February 2000

Abstract

Rapid warm up of an automotive catalyst substrate is important for early light off. This work considers the results from a model of warm up in a single channel. The mass flow is pulsating with high amplitude, about 75% of mean flow, but without flow reversal. The flow regime is laminar within the channel. Pulsations occur with frequency in the range 16–100 Hz, and are important in close-coupled systems where the catalyst is located near to the engine and where the rate of rise of gas inlet temperature with time is rapid, about 15 K/s. The use of a single channel model with conjugate heat transfer enables the heat transfer coefficient to be evaluated and compared with results from steady flow simulations. The value of the augmentation factor based on heat flux is found to be less than unity. The value of the augmentation factor based on heat transfer coefficient depends on the method for calculating the mean heat transfer coefficient, but is generally less than unity. The changes caused by pulsations will be small in practical systems. Changes in wall temperature found in the simulations are the result of the cumulative effect of changes in the mass flow rate.

Keywords: Modelling; Single channel; Automotive catalyst; Heat transfer; Warm up; Pulsating flow

1. Introduction

An automotive catalyst substrate consists of a honeycomb of ceramic material or a mesh of metallic material conformed such that the gases from the engine exhaust ports pass through multiple single parallel channels with square or sinusoidal (approximately triangular) cross-section. The channels typically have hydraulic diameters near 1 mm, and there is a fixed number of cells per cm^2, commonly 62. Recently, substrates with as many as 120 cells/cm^2, thinner walls and smaller diameter channels have been developed. The mass flow through a 50 mm diameter section of catalyst is a few g/s in a warming engine. This mass flow divides and typically passes through approximately 1200 channels in this case, so the flow in each channel is laminar. The substrate in real catalyst systems is washcoated with an alumina/ceria material, which in turn supports the precious metal catalyst. The presence of the washcoat reduces the channel diameter and increases the wall thickness and the thermal capacity of the wall.

The catalyst in a vehicle has been placed traditionally under floor, i.e., about 1.2 m downstream of the engine and the exhaust products are ducted to the catalyst through a metal pipe. This pipe itself must be warmed when the engine is turned on from cold. This delays the warming of the catalyst. The under floor catalyst sees a slow rate of rise of inlet temperature, about 4 K/s, until the light off temperature (in the region of 550 K) is reached. In this period of time while the catalyst is warming, unconverted pollutants from the engine pass out of the vehicle exhaust. In an attempt to speed up the warm up process and thereby reduce the escape of unconverted exhaust, the catalyst is placed closer to the engine. A close-coupled catalyst is only about 0.2 m downstream of the engine. As a consequence of the reduced thermal mass of the pipework between the engine and catalyst, the close-coupled catalyst experiences a higher rate of rise of gas temperature at its inlet. The rate of rise is in the region of 15 K/s averaged over the first 15 s of warm up.

The close-coupled catalyst will also experience pulsations in mass flow because of its greater proximity to the engine. Typically for a four-cylinder engine, an engine speed of 500 rpm causes 16.7 Hz pulsations, and an engine speed of 3000 rpm causes 100 Hz pulsations. This indicates the range of frequency of interest for warm up with pulsating flow. The amplitude of the mass flow pulsations is high, about 75% of the mean flow or greater, but there is generally no flow reversal. The studies discussed here have considered mainly frequencies of 40 Hz and 64 Hz, but 16 Hz has also been investigated. In these studies, the mean mass flow was equivalent to 6.5 g/s through a 50 mm diameter substrate. The pulsation amplitude was typically 5 g/s (77% of mean), with a maximum amplitude of 5.8 g/s (89% of mean) being considered.

* Corresponding author.

E-mail addresses: s.benjamin@coventry.ac.uk (S.F. Benjamin), c.roberts@coventry.ac.uk (C.A. Roberts).

0142-727X/00/$ - see front matter
PII: S0142-727X(00)00025-4

Notation

A_v	wetted surface area per unit bulk volume of substrate, m^2/m^3
A	cross-section area of channel cell, m^2
Aug	augmentation factor
C	half cell thickness of 12th gas cell adjacent the wall
C_{pg}	specific heat of gas, J/(kg K)
C_w	specific heat of substrate wall material, J/(kg K)
CFD	computational fluid dynamics
h	heat transfer coefficient, $W/(m^2K)$
h_{alt}	heat transfer coefficient calculated from Eq. (8), $W/(m^2K)$
k_g	thermal conductivity of gas, W/(mK)
$k_{z,r}$	thermal conductivity of substrate wall material, W/(mK)
m_g	mass flow rate of gas per unit inlet face area, $kg/(m^2s)$
N	number of equispaced time steps during pulsation cycle, typically 40
Q	thermal flux, $W/(m^2K)$
r	radial co-ordinate
R	channel radius, m
t	time, s
Δt	time interval, s
T	period of pulsation frequency, s
T_{bulk}	bulk temperature of gas defined by Eq. (5), K
T_g	temperature of gas, K
T'_g	fluctuating component of gas temperature, K
T_{gin}	temperature of gas at inlet to substrate, K
T_{gout}	temperature of gas at outlet from substrate, K
T_{gm}	mean temperature of gas, K
T_w	temperature of substrate wall, K
T_{wi}	initial temperature of substrate wall, K
T_{wf}	final temperature of substrate wall, K
T_{wm}	spatial mean temperature of substrate wall, K
U	instantaneous velocity of gas flow in z-direction, m/s
U_m	mean velocity of gas flow in z-direction, m/s
U'	fluctuating component of velocity of gas flow in z-direction, m/s
z	Cartesian co-ordinate
Δz	length of element of substrate, m
ϵ	porosity of substrate
ρ	density of material of substrate wall, kg/m^3
ρ_w	$[(1-\epsilon)\rho]$, bulk density of material of substrate walls, kg/m^3
ρ_g	density of gas, kg/m^3
ξ	rate of rise of gas inlet temperature with time, K/s
n	cell number, from 1 to 12
(CA)	time average over the steps of the pulsation cycle, e.g., $B(CA) = (1/N)\sum_{i=1}^{i=N} B_i$
(MWCA)	mass weighted cycle average, see Eq. (9)

The channel cross-section of a single channel in a catalyst substrate is generally square or sinusoidal. When the washcoat layer is added the cross-sectional shapes are modified, for example, the corners of the square channels become rounded. CFD modelling of the detail of the geometry for fluid flow and heat transfer studies in single channels is computationally very demanding, with large numbers of cells required (Day et al., 1999). As an aid to model development, a simpler model was used. The single channel model used in this work was a 30 mm length wedge. The wedge cross-section was a 5° sector of a 1 mm diameter idealised circular channel. The wall properties were those of ceramic with a washcoat layer. The model was thus simple with only 612 finite volume cells and therefore was computationally undemanding. The CFD package STAR-CD was used to solve the equations. The values of T_{bulk} (mass flow weighted mean gas temperature), T_w (wall surface temperature), heat flux at the wall and heat transfer coefficient were deduced. These values were provided at stages through the cycle in the pulsating runs, using either 10, 40 or 100 time steps per cycle. The averaging method was important in the pulsating flow calculations for determining the mean values for the cycle.

If values for heat transfer coefficient can be found from the single channel model, either a complex model (Day et al., 1999) or the more simple model studied here, then they can be applied to a model using the porous medium equivalent continuum approach utilised by Benjamin and Roberts (1998, 1999). In the porous medium approach, the whole system can be modelled but without geometrical detail of the structure of the individual channels. The porous medium model is a way of currently dealing with whole systems under steady flow conditions, without excessive computational demands, but requires knowledge of appropriate heat transfer coefficients. One possible strategy for simulation of pulsating flow would be to use steady flow analysis with augmented heat transfer coefficients. This would be advantageous because of the longer time steps and reduced number of computations required with steady flow analysis.

There is a substantial amount of work reported in the literature on the effects of pulsations on heat transfer. In some studies it is the temperature that oscillates rather than the mass flow, and some studies have investigated frequencies which are very much lower than those of interest here. Some of the reported studies deal with turbulent flow or with situations where there is flow reversal, which generally is not the case in automotive catalysts. Kim et al. (1993) briefly review the literature on heat transfer in pulsating flow and comment on the conflicting results in previous work. Their own work investigated fully developed pulsating flow in a channel. The pulsating flow was of constant temperature at inlet. The wall temperature was uniform and the wall was heated and maintained at a fixed temperature so that heat transferred to the gas. They found that the impact of pulsations on Nusselt number at far downstream locations was minor, but they found enhancement or reduction at other points, dependent upon axial location. They later reported a similar study (Kim et al., 1994) but where a porous medium was placed between the channel walls. In that study they noted a reduction in heat transfer in the entrance region and enhancement further downstream.

The case of catalyst substrate warming by the exhaust products from the engine is a specific problem. The transfer of heat is from the gas to the wall and the inlet gas temperature rises with time. The inlet mass flow is pulsating. The situation is neither one of constant flux nor constant wall temperature; the conditions are transient. It is this particular problem which is studied in this paper using the single channel approach.

2. Theoretical considerations

2.1. Simple analysis (lumped capacitance)

Thermally transient non-pulsating warm up of a solid by a gas may be considered firstly as a lumped capacitance problem.

For an element of length Δz of the catalyst substrate in a short time interval Δt, the following is approximately true if conduction is neglected:

$$hA_v(T_{gm} - T_{wm}) = \rho_w C_w (T_{wf} - T_{wi})/\Delta t = m_g C_{pg}(T_{gin} - T_{gout})/\Delta z,$$

where h is an averaged heat transfer coefficient. The fall in gas temperature as it passes through the catalyst is related to the rate of rise of the wall temperature, and the lag between the gas and wall temperatures is determined by the heat transfer coefficient. After the initial stages of warm up, i.e., typically after about 10 s, the gradient of the gas temperature along the length of the catalyst channel has been shown (Benjamin and Roberts, 1999) to be

$$\frac{dT_g}{dz} = -\frac{\xi \rho_w}{m_g}\frac{C_w}{C_{pg}}. \quad (1)$$

In steady flow cases, the gradient of T_g is steep for low mass flow rates, high wall thermal capacities, just downstream of the substrate inlet at low times and when the rate of rise of gas inlet with time is high, which is the case with close-coupled catalysts. The dependence of this gradient on the reciprocal of the mass flow rate will be important for pulsating flow, where the mass flow rate passes through a large range of values every cycle.

2.2. Full analysis for single channel via CFD simulation

The problem is more completely expressed in terms of two simultaneous equations, in the gas and in the solid. The coordinate system is set up so that the channel axis and flow are in $+z$-direction. The conduction equation for the substrate wall is

$$k_z \frac{\partial^2 T_w}{\partial z^2} + \frac{k_r}{r}\frac{\partial}{\partial r}\left[r\frac{\partial T_w}{\partial r}\right] = \rho C_w \frac{\partial T_w}{\partial t}. \quad (2)$$

The energy equation describing the gas is

$$k_g \frac{\partial^2 T_g}{\partial z^2} + \frac{k_g}{r}\frac{\partial}{\partial r}\left[r\frac{\partial T_g}{\partial r}\right] = \rho_g C_{pg}\left[\frac{\partial T_g}{\partial t} + U\frac{\partial T_g}{\partial z}\right]. \quad (3)$$

At the interface between the gas and the wall, the boundary condition is that the heat flux is continuous

$$Q = -k_g \left.\frac{\partial T_g}{\partial r}\right|_{r=R} = -k_r \left.\frac{\partial T_w}{\partial r}\right|_{r=R}.$$

In the case of pulsating flow, the inlet boundary condition is of the form velocity $U = U_m + U'$ where the magnitude of U' is similar to U_m. The gas temperature and its gradient will also be periodic when the equations are solved. Thus there is an extra and significant term in Eq. (3), namely

$$\rho_g C_{pg}\, U' \frac{\partial T'_g}{\partial z}. \quad (4)$$

The commercial CFD program STAR-CD can be used to solve Eqs. (2) and (3) simultaneously. Fig. 1 shows a mesh diagram of the simple cell structure of the 5° wedge-shaped portion of the idealised single channel. The mesh is one-cell thick and so the problem is dealt with as a 2D axially symmetric case. The two large surfaces of the wedge are treated as symmetry planes. There is 4 mm length of fluid duct at inlet upstream of the channel. There are three cells of washcoat and three cells of wall where the duct diameter is reduced for the 30 mm length of the channel. There are 30 cells along the length of the channel, of which the first six are 0.5 mm in length. The final three cells at the outlet of the channel are 2 mm in length. The rest of the cells are 1 mm in length. The high aspect ratio of the cells was found to be satisfactory for the predominantly 1D flow. The twelve cells which are spaced across the radius of the channel are sized to have equal cross-sectional area as this simplifies the bulk averaging calculations. The inlet boundary condition is either a constant or a pulsating spatially uniform mass flow of gas with its temperature rising with time. The outlet boundary is 30 mm downstream of the channel inlet and is at atmospheric pressure. The outer wall of the model (i.e., mid point of the channel wall) is adiabatic. The initial condition is that the system contains fluid at 299 K, but the walls are at 293 K. The inlet (impinged) face of the solid substrate and the length of the wall in contact with the fluid are conjugate heat transfer surfaces where there is continuity of heat flux. The downstream facing wall adjacent the channel outlet is adiabatic. The flow regime is laminar.

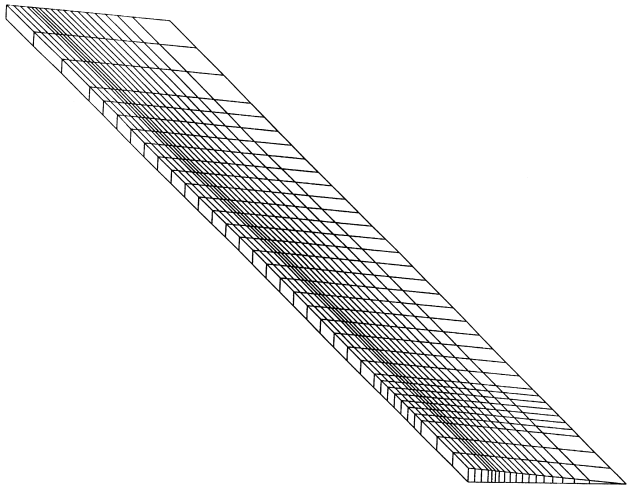

Fig. 1. Mesh used for single channel CFD simulation.

The SIMPLE algorithm was used to obtain a converged solution for a cold flow steady-state case. The transient cases were restarted from this converged solution. The PISO algorithm and upwind differencing for all variables, except density, were used for the numerical computations in the transient cases. The convergence criteria for the PISO algorithm were the default values for the STAR-CD package, which are appropriate for almost all transient cases. In Section 3 below the significance of the time step in transient cases is discussed. Double precision was used for the computations. Use of upwind differencing was justifiable for the simple single channel model because the mesh was aligned with the flow. Also, the model featured a relatively high number of cells, and in the early studies the cell lengths were increased from 0.25 to 1 mm without significant change in temperature values. This reduction in the number of cells, together with the use of upwind differencing, meant that the model was stable and ran reliably to provide results fairly rapidly. A refined mesh of 18 cells radially across the channel was investigated to check mesh independence. Numerical changes in results were very small, overall much less than 1%, and the trends observed in flux and heat transfer ratios were unchanged so the 12 cell model was used.

The inlet gas temperature is taken to be $[300 + 4t]$ approximating to the under floor condition or $[300 + 15t]$ approximating to the close-coupled condition. The mean mass flow rate is set as equivalent to 6.5 g/s through a substrate of 50 mm diameter. This corresponds to a Reynolds number in each channel of about 250. Table 1 gives numerical values for the channel dimensions and for the properties of the wall used in these studies.

Table 1
Input data and parameters for simulation of single channel warm up

	Values for washcoated ceramic
Washcoat density (kg/m^3)	1350
Washcoat conductivity (W/(mK))	0.2
Washcoat specific heat (J/(kg K))	950
Ceramic density (kg/m^3)	2500
Ceramic conductivity (W/(mK))	1.4
Ceramic specific heat (J/(kg K))	1100
Channel radius (mm)	0.5093
Washcoat thickness (mm)	0.0447
Wall (half) thickness (mm)	0.081
Nominal cell diameter (mm)	1.27

2.3. Averaging of results

There are 12 cells of equal cross-sectional area A along the single channel radius (see Fig. 1) and the following indicates the averaging method for evaluating T_{bulk} at a defined location z (mm) along the single channel model:

$$T_{\text{bulk}}(z) = \frac{\sum_{n=1}^{12}(\rho_n U_n A T_{gn})}{\sum_{n=1}^{12}(\rho_n U_n A)}. \tag{5}$$

At the wall, the wall surface temperature is assumed to be the value for the first washcoat cell. This implicitly makes the assumption that the temperature gradient in the washcoat cells is negligibly small. The gas temperature of the 12th gas cell is assumed to be the gas temperature at a distance from the wall equal to half the thickness of the 12th gas cell.

Thus, flux Q (W/m^2) is found from

$$\frac{k_g(T_{g12} - T_w)}{C},$$

where gas conductivity k_g is evaluated at the mean of T_{g12} and T_w, and C is the cell half thickness.

Therefore, heat transfer coefficient

$$h\ (\text{W}/(\text{m}^2\text{K})) = \frac{Q}{(T_{\text{bulk}} - T_w)}.$$

The pulsations were input to the simulations as sinusoidal variations in mass flow. The pulsations observed in real engines may vary considerably in form but are very approximately sinusoidal. For comparison with a steady flow of 6.5 g/s, an example of pulsating mass flow input is

$$6.5 + 5.0\sin(2\pi t/T) = 6.5 + 5.0\sin(2\pi I/N),$$

where I is iteration number, N is number of iterations per cycle. The time step fixes the frequency. When time averaging through a pulsation cycle, it is significant that values of $[Q(\text{CA})/[T_{\text{bulk}} - T_w](\text{CA})]$ are significantly different from $[Q/(T_{\text{bulk}} - T_w)](\text{CA})$, where (CA) indicates a time average through the cycle. The latter is the result of averaging the true instantaneous values of h over a cycle.

There are three alternative ways of calculating the cycle-averaged value for heat transfer coefficient h. For steady state the relationship is expressed

$$h_{\text{steady}} = \frac{Q}{(T_{\text{bulk}} - T_w)}. \tag{6}$$

If the instantaneous value for h at an instant during a cycle is calculated from (6) then

$$h_{\text{inst}} = \frac{Q_{\text{inst}}}{(T_{\text{bulk}} - T_w)_{\text{inst}}},$$

$$h(\text{CA}) = (1/N)\sum_{1}^{N} h_{\text{inst}}, \tag{7}$$

where N is the number of equispaced time steps through the cycle at which values are available.

Alternatively, Q and $(T_{\text{bulk}} - T_w)$ can be cycle averaged similarly but independently so that

$$h_{\text{alt}} = \frac{Q(\text{CA})}{[T_{\text{bulk}} - T_w](\text{CA})}. \tag{8}$$

Thirdly, it is possible to average the value for T_{bulk} by mass weighting through the pulsation cycle:

$$T_{\text{bulk}}(\text{MWCA}) = (1/[Nm'(\text{CA})])\sum_{1}^{N}(m' T_{\text{bulk}}) \tag{9}$$

Then

$$h(\text{MWCA}) = \frac{Q(\text{CA})}{T_{\text{bulk}}(\text{MWCA}) - T_w(\text{CA})}. \tag{10}$$

The three values for h from (7) (8) and (10) for cases of pulsating flow are quite different and it is necessary to distinguish between them. Eq. (7) gives the cycle average of the true instantaneous values for h, but Eq. (9) utilises a value for T_{bulk}, the so-called mixing cup temperature, which would correspond with experimental measurements. Augmentation of heat transfer from the steady state to some other condition such as pulsating flow is often defined in terms of the ratio of heat transfer coefficients. Following the discussion above, however, regarding Eqs. (7) (8) and (10), it is considered preferable to define augmentation in terms of heat flux rather than heat transfer coefficient:

$$\begin{aligned} Q &= h_{\text{steady}}(T_{\text{bulk}} - T_w)_{\text{steady}}, \\ Q(\text{CA}) &= \text{Aug}\ h_{\text{steady}}(T_{\text{bulk}} - T_w)_{\text{steady}}, \\ \text{Aug} &= \frac{Q(\text{CA})}{Q}. \end{aligned} \tag{11}$$

3. Results of single channel simulations

The choice of time step for the simulations was made with consideration of the nominal residence time of the gas in the substrate. The number of steps per cycle used for the simulations was either 10, 40 or 100. In fact, the numerical differences in the results obtained were exceptionally small, with 10 steps per cycle being acceptable at 40 Hz. In most runs, however, either 40 or 100 time steps per cycle were used. For a 1 mm length cell and velocity 6 m/s the residence time is 0.17 ms. At 40 Hz, 40 times steps per cycle corresponds to a time step of 0.625 ms. Thus the Courant number is only about 3.5 whereas 50 is acceptable for transient PISO simulations.

3.1. Results for 4 K/s rate of inlet temperature rise

The first results to be discussed are those for inlet gas temperature $300 + 4t$ which corresponds approximately to the condition in an under floor catalyst.

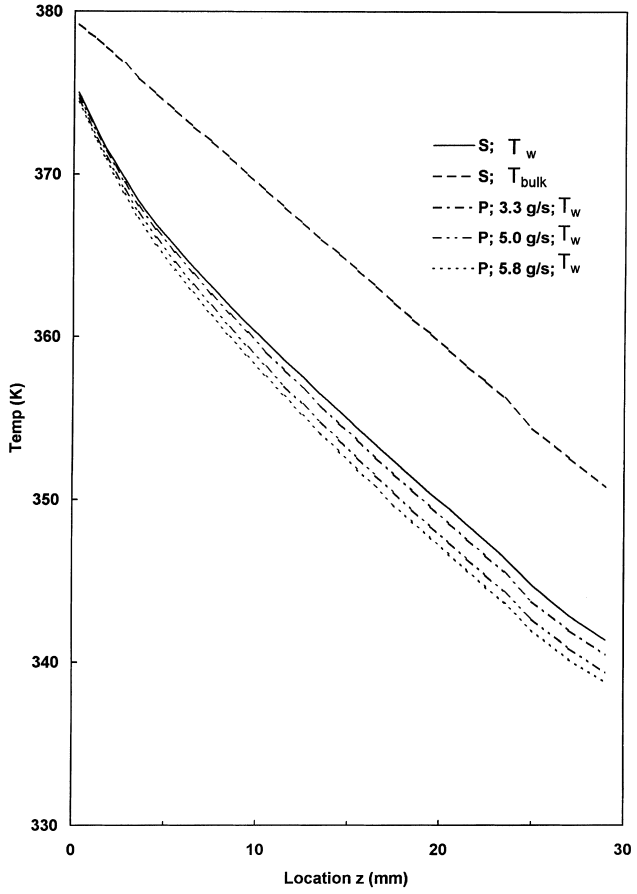

Fig. 2. Effect of pulsating mass flow amplitude on wall temperature at 20 s. Mass flow pulsation amplitudes are shown in the legend. Mean mass flow 6.5 g/s. Frequency 40 Hz. *S* indicates steady flow. *P* indicates pulsating flow.

3.1.1. Effect of pulsation amplitude

Fig. 2 shows the effect of pulsating mass flow amplitude on wall temperature. The simulations were for 40 Hz frequency with 40 time steps/cycle. The mean inlet mass flow was 6.5 g/s, based on a 50 mm diameter catalyst. The temperatures in Fig. 2 are calculated for the end of a pulsation cycle. The wall temperature is not responsive at the frequencies investigated in this study and so the plotted temperature is the same as the cycle averaged wall temperature. The gas temperatures change greatly over the pulsation cycle so only steady T_{bulk} is plotted. The amplitudes investigated are 3.3 g/s (51% of mean), 5.0 g/s (77% of mean) and 5.8 g/s (89% of mean). A consistent trend towards reduced wall temperature with increased pulsating mass flow amplitude can be discerned. Warm up is best achieved by the steady flow.

3.1.2. Effect of pulsation frequency

The effect of pulsating mass flow frequency was investigated. The simulations were for 40 times steps/cycle. Fig. 3 shows the ratio of the cycle averaged mean heat flux at the wall to the steady flow heat flux. The values are at 5 s for frequencies in the range 16–64 Hz. It can be seen that the flux is less in the lower frequency cases. At 64 Hz the reduction from the steady flow case is at most about 5% and at 16 Hz the reduction is about 7%.

3.1.3. Effect on heat transfer coefficient

The effect of 40 Hz mass flow pulsations on the heat transfer coefficient was investigated. The runs were for mean mass flow 6.5 g/s with 5.0 g/s pulsation amplitude. There were 40 time steps per cycle. The cycle-averaged value for h from Eq. (7) and the steady flow value for h were found to be very similar. When h is calculated from Eq. (8), however, where $(T_{bulk} - T_w)$ is a simple time average, not mass flow weighted, a small increase $< 2\%$ in h is found. In practical terms changes of this order would not cause significant changes in predictions from the porous medium (equivalent continuum) model (Benjamin and Roberts, 1998, 1999). Fig. 4 plots h ratios and shows that the augmentation factor for heat transfer coefficient with pulsations is <1 in the first few mm of the channel. It is

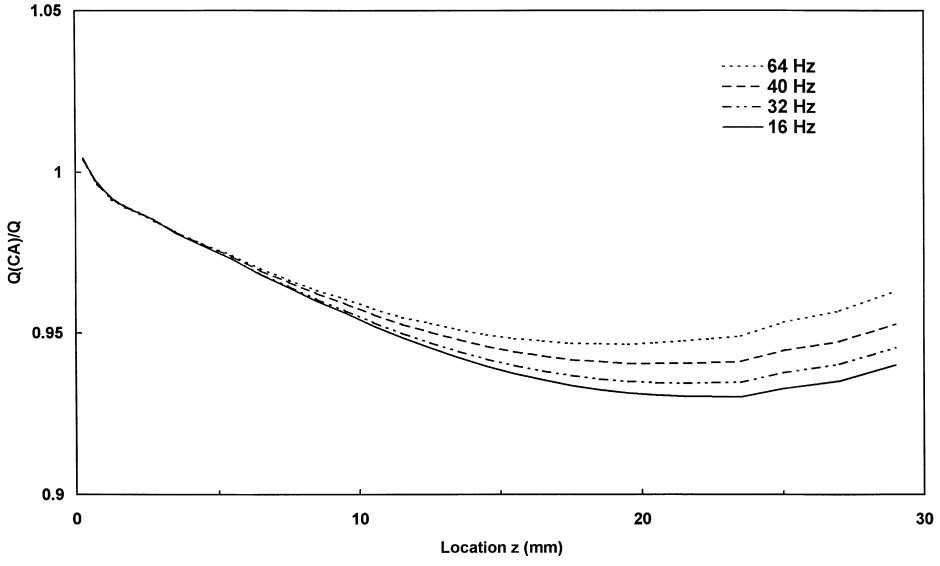

Fig. 3. Ratio of heat flux in pulsing and steady simulations at 5 s. Frequencies are shown in the legend. Pulsating mass flow 6.5 ± 5.0 g/s.

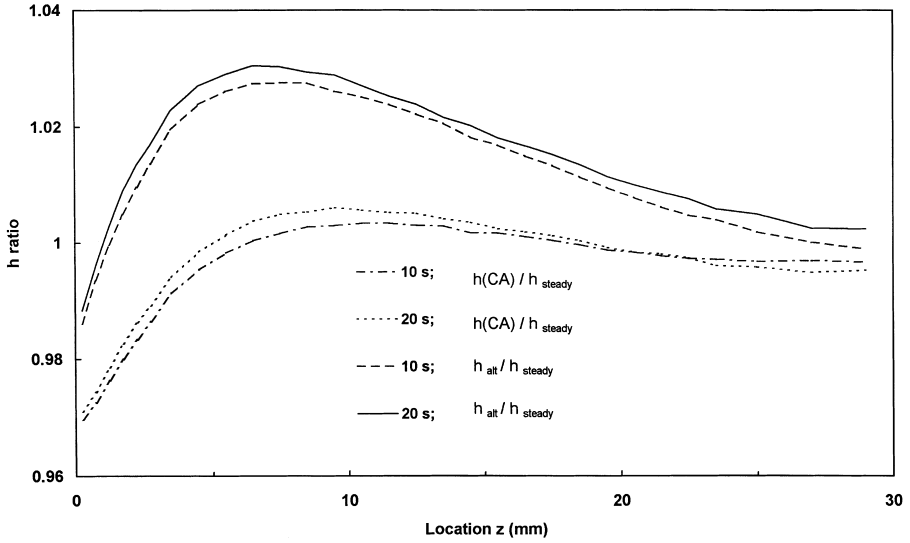

Fig. 4. Ratio of heat transfer coefficient from pulsating flow to steady flow simulations. Value for h(CA) is from Eq. (7); value for h_{alt} is from Eq. (8).

then greater than 1 for a few mm but then returns to a value near unity.

Fig. 5 shows values for the ratio $Q(\mathrm{CA})/Q$ up to 20 s. It is clearly seen that with pulsations, the heat flux from the gas to the wall is reduced. Thus the steady flow situation is the optimum for warming the substrate. The cycle-averaged flux is most greatly reduced in the first few seconds of warm up; it is reduced by $< 5\%$ after 10 s.

Comparing Figs. 4 and 5, and referring to the equations in Section 2.3, it is apparent that it is not possible by simply changing the value for h in a steady flow run to correctly predict both Q and $(T_{\mathrm{bulk}} - T_{\mathrm{w}})$ for pulsating mass flow. The differences are in practical terms, however, very small. Thus it may be acceptable to use steady flow analysis in the substrate itself for prewarming predictions under conditions of pulsating flow when the inlet temperature ramp is about 4 K/s and the mass flow amplitude is about 77% of mean.

3.2. Results for 15 K/s rate of inlet temperature rise

The results now to be discussed are those for inlet gas temperature $300 + 15t$, which corresponds approximately to the conditions in a close-coupled catalyst. More significant effects may be expected with this steeper temperature inlet ramp if the gradient of gas temperature along the length of the substrate varies widely over each cycle of pulsation, see Section 2.1.

3.2.1. Comparison of cycle averaged values with steady flow values

Fig. 6 shows the effect of inlet temperature rise, 5, 10 and 15 K/s, for a mean flow of 6.5 g/s, amplitude 5 g/s, and frequency 16 Hz. The value for $Q(\mathrm{CA})/Q$(Steady) can be seen to vary only slightly with the rate of rise of inlet temperature. The

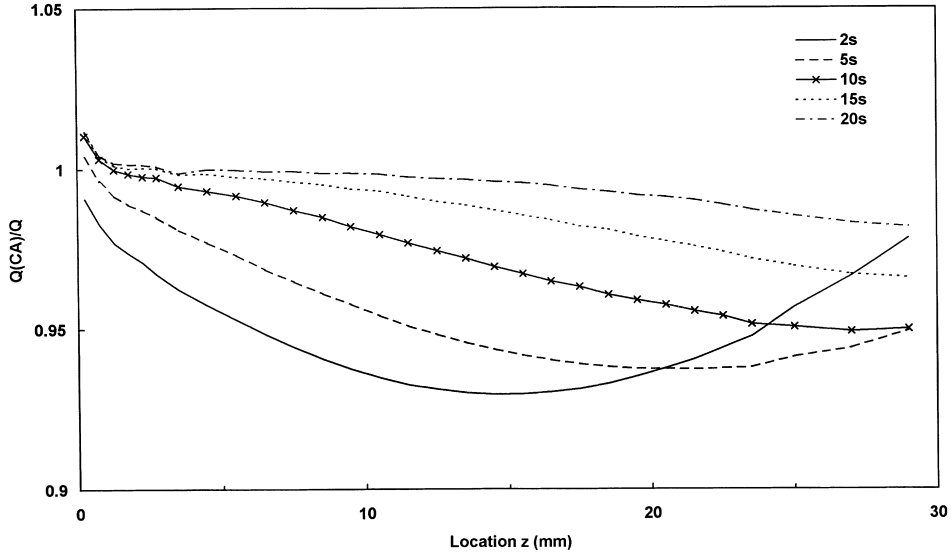

Fig. 5. Ratio of heat flux from 40 Hz pulsating flow to steady flow. Pulsating mass flow 6.5 ± 5.0 g/s.

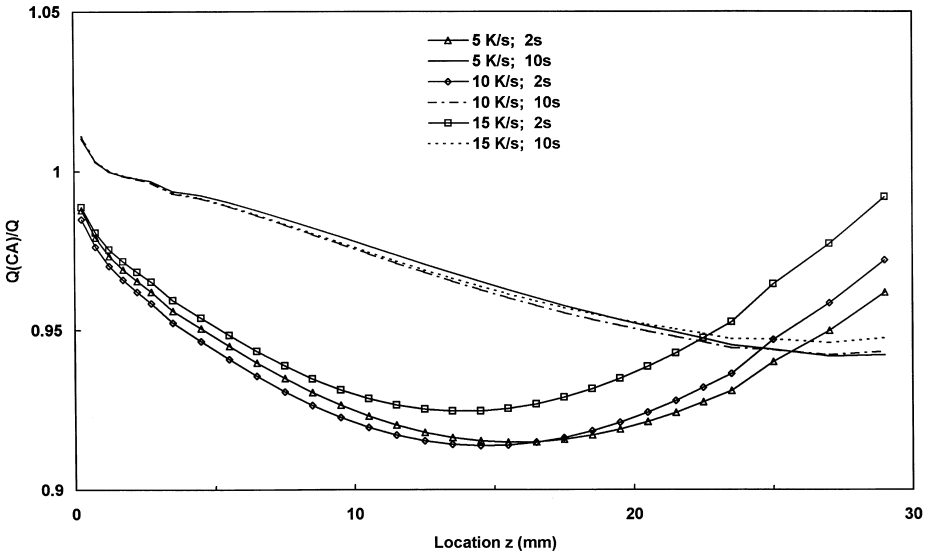

Fig. 6. Effect of inlet temperature ramp, shown in legend, on ratio $Q(CA)/Q$ at times 2 s and 10 s for mean mass flow 6.5 g/s. When pulsing, frequency is 16 Hz and mass flow amplitude 5.0 g/s.

effect is smaller than that of mass flow amplitude, which is clearly demonstrated in Fig. 7.

Fig. 8 shows the cycle-averaged values of T_{bulk} (mass flow weighted) and T_w for the case with frequency 16 Hz, amplitude 5.8 g/s, and 15 K/s rate of rise at inlet compared with the steady flow values. The pulsating flow can be seen to have reduced the wall temperature by almost 10 K at 20 s at about 20 mm from the inlet. This is a significant effect that could influence the onset of light off in this region. The average bulk gas temperature over the cycle, weighted for mass flow changes through the cycle, is seen to be above the steady flow gas temperature towards the tube exit, most notably at low times. Fig. 9 shows the effect of pulsations on the heat flux at the wall for this particular case at times from 2 to 20 s. In Fig. 9, for example, there is a 10% reduction in flux in the pulsating case at 2 s at about 12 mm from the channel inlet. Figs. 6 and 7, however, have demonstrated that mass flow amplitude is more influential than inlet temperature rate of rise. If Fig. 9, effectively the close-coupled case, is compared with Fig. 5, effectively an under floor case, the differences noted are due to mass flow amplitude (effect shown in Fig. 7) and frequency (effect shown in Fig. 3) rather than inlet temperature rise (effect shown in Fig. 6). Thus when simulating a close coupled catalyst, it is the higher mass flow amplitude, rather than the higher rate of rise of inlet temperature, which will be significant.

Fig. 10 shows heat transfer coefficient ratios plotted in the same way as Fig. 4, with the addition of the ratio calculated from Eq. (10). It can be seen that the differences between $h(\mathrm{CA})$ and h_{steady} and between h_{alt} and h_{steady} are slightly greater in Fig. 10, for 15 K/s inlet ramp, 5.8 g/s amplitude and 16 Hz, than in Fig. 4, for 4 K/s inlet ramp, 5 g/s amplitude and 40 Hz. In Fig. 10, $h(\mathrm{CA})$ is reduced to 98.5% of its steady value for z

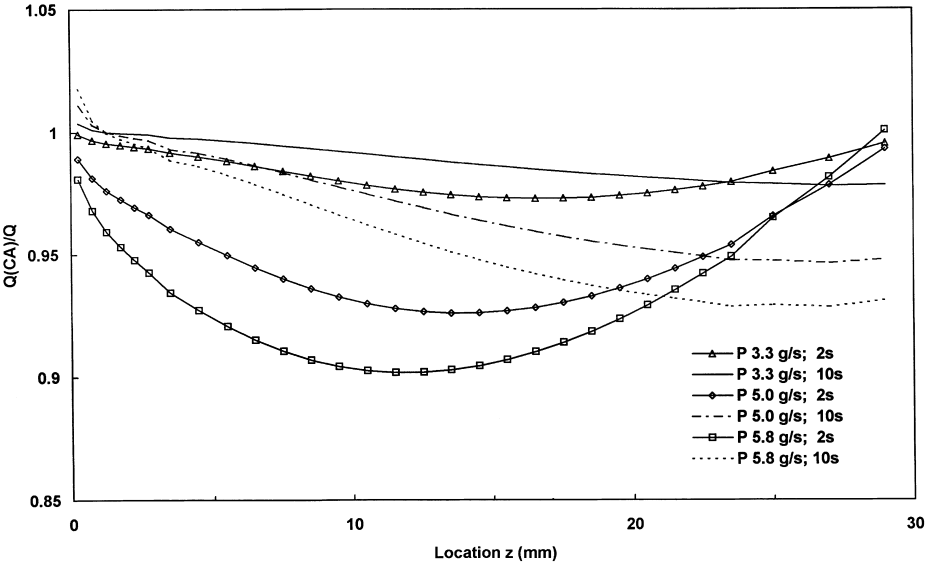

Fig. 7. Effect of mass flow pulsation amplitude, shown in legend, on ratio $Q(\mathrm{CA})/Q$ at times 2 s and 10 s for 16 Hz pulsations about a mean mass flow of 6.5 g/s and with $300 + 15t$ gas inlet temperature.

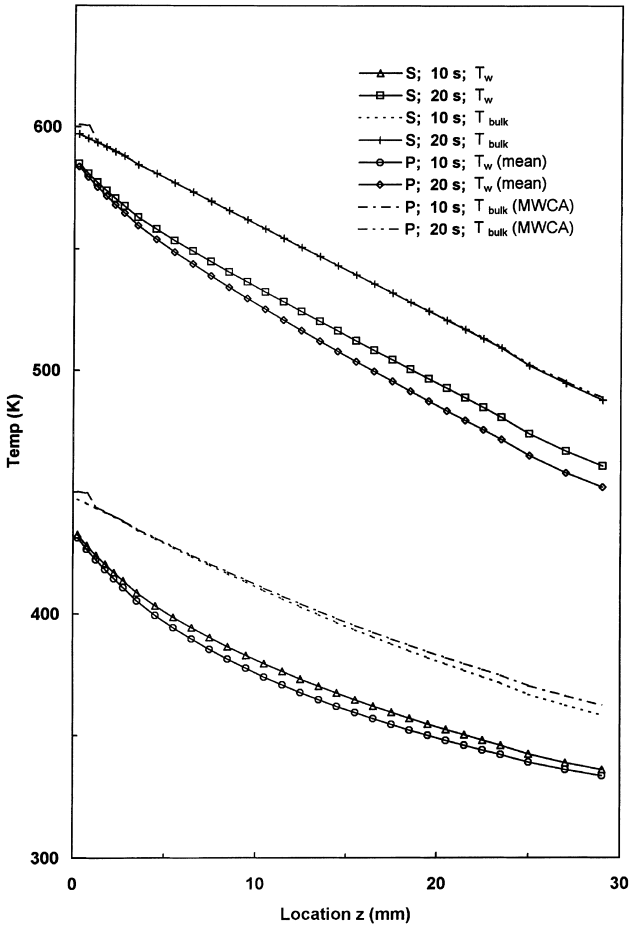

Fig. 8. Cycle averaged mean temperatures for 16 Hz pulsing flow 6.5 ± 5.8 g/s compared with steady flow. Inlet temperature $300 + 15t$. Plotted for 10 s and 20 s. *S* indicates steady flow. *P* indicates pulsating flow.

near 25 mm after 10 s; but this figure shows that the values for h(MWCA) from Eq. (10), are much more significantly different, with h(MWCA) being reduced to 70% of the steady value at 30 mm from the channel inlet. Even these larger changes between the steady case and the pulsating case noted in Fig. 10 when h is calculated in this way are, however, still relatively small. They would be expected to have only a moderate influence on predictions of solid temperatures from the porous medium (equivalent continuum) model (Benjamin and Roberts, 1998).

3.2.2. Comparison of effect of pulsating flow with steady mass flow of lower value

The significant temperature changes noted in Fig. 8 are the result of the cumulative effect of varying mass flow through the pulsation cycle. One way of interpreting these changes is by use of an effective heat transfer coefficient. An alternative is to interpret the cumulative effects of the pulsating mass flow, as being caused by an effective mass flow which is lower than the mean of the pulsating mass flow. In Section 2.1 it is indicated that the temperature gradient along the length of the channel is inversely proportional to mass flow rate m_g under steady flow conditions. The mean temperature gradient over the cycle might therefore be expected to correspond to an equivalent mass flow rate that is based on the mean of $(1/m_g)$. This equivalent mass flow rate is much lower than mean m_g. Fig. 11 shows the gas and wall temperatures at 15 s for a pulsating flow 6.5 ± 5.8 g/s at 16 Hz compared with steady flows of 5.2 g/s, 5.85 g/s and 6.5 g/s. It can be seen that the wall temperatures for the pulsating flow case are well predicted by the run for 5.85 g/s steady flow. There is a discrepancy in the gas temperatures, as would be expected, but it is the prediction of the wall temperature which is significant for the prediction of light off. The heat flux for the pulsating case can be compared with the three steady flow cases and it is also found to be approximated by the heat flux in the 5.85 g/s steady flow case.

4. Conclusions

This work has investigated the significance of pulsations by using a single channel model. Close-coupled and under floor

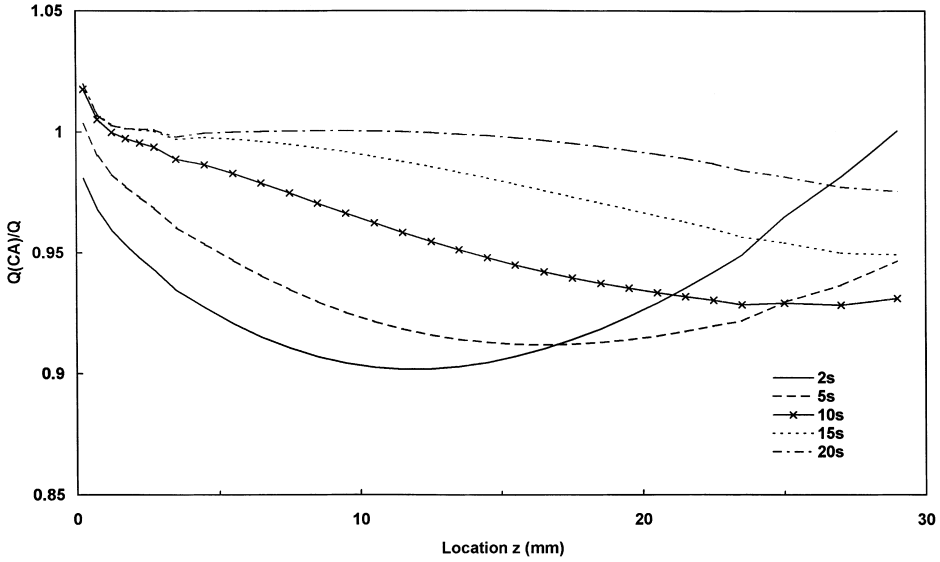

Fig. 9. Ratio of heat flux from 16 Hz pulsating flow and steady flow simulations at times shown in legend. Mass flow 6.5 ± 5.8 g/s. Gas inlet temperature $300 + 15t$.

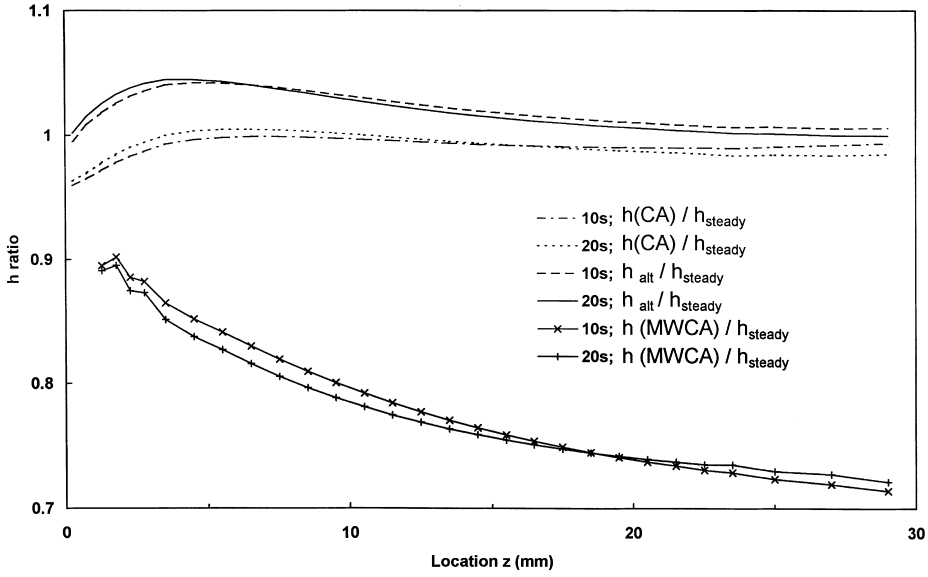

Fig. 10. Ratio of heat transfer coefficient for pulsating flow to steady flow. Frequency 16 Hz, mass flow 6.5 ± 5.8 g/s, gas inlet temperature 300 + 15*t*. Value for *h*(CA) from Eq. (7), for h_{alt} from Eq. (8) and for *h*(MWCA) from Eq. (10).

catalysts are likely to see different rates of temperature rise at inlet and different amplitudes of mass flow pulsation. Generally, pulsations are likely to be of higher amplitude for close-coupled catalysts, although acoustic tuning can increase the magnitude of the pulsations even for under floor converters.

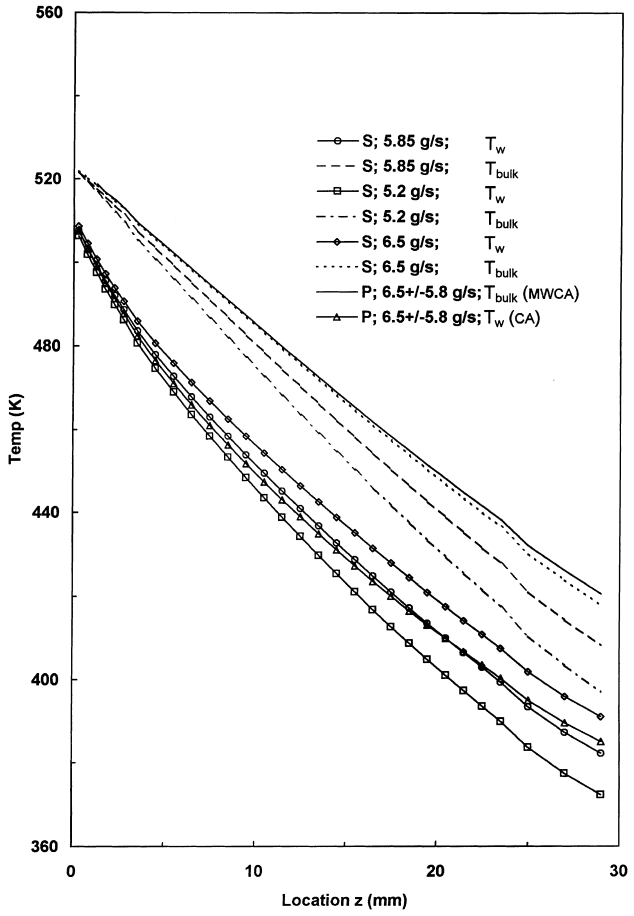

Fig. 11. Comparison of wall and gas temperatures obtained at 15 s for pulsating (*P*) mass flow 6.5 ± 5.8 g/s and for three different steady (*S*) flows for gas inlet temperature 300 + 15*t*.

With pulsating mass flow, the computations have shown that amplitude has an influence. A higher pulsating mass flow amplitude causes lower wall temperatures. The wall temperature does not respond during the cycle at the frequencies investigated. The highest amplitude investigated was 89% of the mean which reduced the wall temperatures by several degrees when the inlet temperature rose by 4 K/s and the pulsation frequency was 40 Hz.

The results also suggest that frequency is influential but with a less significant effect than amplitude. Lower frequencies are seen to be more effective in reducing heat flux, but very low frequencies < 16 Hz where this effect may become more important are generally not of interest for automotive exhaust systems.

Various rates of temperature rise at inlet were investigated, with 4 K/s corresponding to the under floor condition and 15 K/s to close coupling. In a case where the rate was 15 K/s, frequency 16 Hz and amplitude 5.8 g/s about a mean of 6.5 g/s, some fairly significant reductions in wall temperature, approaching 10 K, were noted by 20 s after the start of warm up. Changes of this order may influence the onset of light off.

The results obtained support the use of steady analysis in the substrate itself for the prediction of catalyst prewarming by pulsating flow prior to light off only if certain conditions are met. These are that the mass flow pulsation amplitude is low, less than 80% of the mean, and the frequency is in the normal range, not excessively low. These conditions are more likely to be realised under floor. The augmentation factor for heat flux is between 0.9 and unity in the catalyst itself in the cases presented in this paper. If augmentation is in the upper part of this range, some error will be introduced by using steady state analysis to simulate pulsating flow conditions but there will be a large reduction in computations required, which is advantageous. This may not be acceptable, however, in the cases where the augmentation is closer to 0.9. The effects on wall temperatures caused by the pulsating flow can be significant, as shown in Fig. 8, and a steady flow run at the mean mass flow rate would not be a close enough approximation in this case. It is possible, however, to simulate wall temperatures under such pulsating conditions by a steady flow simulation but using a

reduced mass flow rate. This predicts the bulk gas temperatures incorrectly, but the wall temperatures which are required are well predicted and there is a considerable saving in computational effort.

Pulsations have been shown to influence the value of heat transfer coefficient value in a single channel, dependent upon the averaging method used, and they have been shown to influence temperature, particularly in the case where amplitude of pulsation is high. The effects are the result of the cumulative influence of changes in mass flow rate. It is also likely that the presence of pulsations will alter the flow and temperature patterns in the expander cone (diffuser) upstream of the catalyst in a real exhaust system. This will in turn change the inlet boundary condition to the catalyst itself from the situation with steady flow to a different situation with pulsating flow. In this way the behaviour of a real system will be further altered under pulsating flow conditions. It is also probable that the presence of pulsations will alter the diffusional and chemical processes that occur in a single channel around light off time. These additional issues will define the scope of the future work programme which aims to predict processes in the catalyst beyond the early stages of warm up which are considered in this paper.

Acknowledgements

The authors acknowledge Arvin Exhaust Ltd., Ford Motor Co., Jaguar Cars Ltd. and Johnson Matthey plc, whose generous financial support and technical advice have enabled this project to proceed. Also, the authors acknowledge the SERC/DTI Link Programme on Applied Catalysis, which is currently funding this project.

References

Benjamin, S.F., Roberts, C.A., 1998. Warm up of automotive catalyst substrates: comparison of measurements with predictions. Int. Comm. Heat Mass Transfer 25 (1), 19–32.

Benjamin, S.F., Roberts, C.A., 1999. Modelling warm up of an automotive catalyst substrate using the equivalent continuum approach. Int. J. Vehicle Design 22 (3/4), 253–273.

Day, E.G.W., Benjamin, S.F., Roberts, C.A., 1999. Single channel studies of heat transfer in automotive catalyst converters 4th IMechE/SAE Vehicle Thermal Management Systems Conference Proceedings, VTMS-4, pp. 347–363.

Kim, S.Y., Kang, B.H., Hyun, J.M., 1993. Heat transfer in the thermally developing region of a pulsating channel flow. Int. J. Heat Mass Transfer 36 (17), 4257–4266.

Kim, S.Y., Kang, B.H., Hyun, J.M., 1994. Heat transfer from pulsating flow in a channel filled with porous media. Int. J. Heat Mass Transfer 37 (14), 2025–2033.